Electronic properties of transition-metal oxides under high pressure revealed by x-ray emission spectroscopy

2005 J. Phys.: Condens. Matter 17 S717

(http://iopscience.iop.org/0953-8984/17/11/001)

INSTITUTE OF PHYSICS PUBLISHING JOURNAL OF PHYSICS: CONDENSED MATTER

J. Phys.: Condens. Matter **17** (2005) S717–S726 doi:10.1088/0953-8984/17/11/001

Electronic properties of transition-metal oxides under high pressure revealed by x-ray emission spectroscopy

J-P Rueff[1], **A Mattila**[2], **J Badro**[3], **G Vankó**[4] **and A Shukla**[3]

[1] Laboratoire de Chimie Physique—Matière et Rayonnement, 11 rue Pierre et Marie Curie, 75231 Paris Cedex 05, France
[2] Division of X-Ray Physics. Department of Physical Sciences, PO Box 64, 00014 University of Helsinki, Finland
[3] Laboratoire de Minéralogie Cristallographie Paris, Université Paris 6, 4 place Jussieu, 75252 Paris Cedex 05, France
[4] European Synchrotron Radiation Facility, BP 220, 38043 Grenoble, France

Received 5 January 2005
Published 4 March 2005
Online at stacks.iop.org/JPhysCM/17/S717

Abstract

The high-pressure electronic and magnetic properties of MnO, CoO and NiO have been investigated by x-ray emission spectroscopy. Both MnO and CoO show a magnetic collapse revealed by the abrupt decrease of the satellite intensity in the metal Kβ emission lines at about 80 and 100 GPa respectively. The magnetic transition pressures agree well with the known structural transition pressures in these systems. No such magnetic transition was observed in NiO, which rather shows hints of delocalization of the d electrons. The NiO data have been further analysed within a full multiplet approach. The low- and high-pressure emission spectra could be reproduced well. The confrontation between theory and experiment gives a handle on fundamental quantities such as the electron correlation strength, hybridization and charge transfer energy, introduced in the calculations as parameters. Both theoretical and experimental clues indicate that NiO is on the verge of a metal–insulator transition. In MnO and CoO, the magnetic transition is likely to arise from the interplay between the ligand field and the O p bandwidth.

(Some figures in this article are in colour only in the electronic version)

1. Introduction

Transition-metal oxides constitute a fundamental class of materials embracing a vast variety of remarkable phenomena among which are strong electron correlations, charge transfer, charge or orbital ordering and itinerant magnetism (see Imada *et al* for a recent review [1]). In this complicated picture, pressure plays a crucial role since it can alter the d electronic density and hybridization, and thereby the localization of the d electrons and their magnetic properties. At

the very core of metal oxide properties under high pressure reside the notions of metal–insulator transition (MIT) and magnetic collapse.

1.1. Magnetic collapse

Back in the 1950s, Mott had already pointed out the tight relationship between the insulating state of transition-metal compounds and electronic density [2]. When the atoms are sufficiently separated, the on-site Coulomb interaction acting between the d electrons opens a gap in the d density of states; in fact, in most transition-metal oxides, the correlation gap is controlled by the charge transfer energy Δ necessary to promote an electron from the oxygen ligand to the metal atom. The insulating character persists upon increasing the density (i.e. pressure) until the screening becomes effective enough to destroy the electronic correlation that maintains the insulating state, while the d bandwidth increases due to the growing band overlap. As a consequence, the system undergoes a first-order insulator–metal transition, which is usually accompanied by a magnetic collapse of the transition metal. Here, the disappearance of the d magnetic moment (and not only the long-range magnetization) results from the progressive delocalization of the d electrons.

Magnetic collapse can be more simply sketched within an atomic picture. As we will discuss hereafter, the atomic picture is most useful when discussing the x-ray emission data on the transition-metal oxides. Most of the metal oxides crystallize at ambient pressure in the rock-salt NaCl-like (B1) structure, consisting of two interlaced fcc lattices composed of oxygen and metal ions. Note that the onset of antiferromagnetic order at T below T_N may lead to a rhombohedral distortion of the unit cell (rB1), characterized by a slight compression along the cube diagonal. For simplicity, in the following we will consider the transition-metal ions to sit in non-distorted octahedral sites surrounded by six oxygen neighbours. In the O_h symmetry, the ligand field splits the d band into two subbands t_{2g} and e_g having sixfold and fourfold degeneracy respectively. At ambient conditions, the d band is spin polarized and the majority and minority band are split by the exchange interaction J. When pressure is applied, the ligand field strength increases as a result of the M–O distance shortening. In contrast, J, an intra-atomic property, remains constant. At a given pressure, the ligand field strength $10Dq$ will overcome the magnetic exchange interaction and the magnetism will be suppressed. In this simplistic picture, the magnetic collapse therefore results from a competition between the crystal field and magnetism (exchange interaction), while it stems rather from the interplay between the d–d Coulomb interaction U and d bandwidth W in the strongly correlated electron scheme.

Most of the investigations of the magnetic state of metal oxides under pressure have been carried out over the past year principally via Mössbauer spectroscopy [3–5] or x-ray magnetic dichroism [6, 7]. Besides these techniques, we have recently developed the use of x-ray emission spectroscopy (XES) as an alternative probe of the transition-metal magnetism [8–10]. XES is well suited to high-pressure studies thanks to the intense fluorescence yield in the hard x-ray energy range, especially when combined with bright and focused x-ray beams provided by third-generation synchrotron sources. More particularly, the Kβ emission line turns out to be extremely sensitive to the transition-metal spin state.

1.2. XES at the Kβ line

The x-ray emission results from the radiative decay of an excited atom after primary excitation far from resonance. Here, we will focus more particularly on the Kβ emission line ($3p \rightarrow 1s$) from the transition-metal atom. In the XES final state, the interaction of the 3p core hole

with the 3d electrons leads to a splitting of the emission line into many components. Notably, the 3p–3d exchange interaction is responsible for the growth of a satellite structure on the low-energy side of the emission line. We consider various parameters such as the metal formal oxidation state and the degree of covalency of the metal–ligand bond; among these, the satellite intensity and its separation in energy from the main peak mainly depend on the strength of the 3p–3d exchange interaction [11, 12], and thus indirectly on the 3d magnetic moment. As the 3d magnetic moment is varied, the satellite intensity changes, and one expects it to vanish when a collapse of the magnetic state is attained.

In the present paper, we will review recent XES experiments performed on simple metal oxides under very high pressure. The experimental set-up and XES results will be presented in a first part. The results will be discussed in the second part in the light of recent theoretical progress.

2. Experimental details

2.1. Overall set-up

The experiment was carried out on the inelastic x-ray scattering beamline (ID16) at the European Synchrotron Radiation Facility (ESRF), Grenoble. The beam was monochromatized by a Si(111) two-bounce channel-cut crystal and focused onto the sample position by a toroidal mirror located downstream. The spot size at the sample position is 20(V) $\times$ 80(H) μm^2.

Powdered sample was loaded in a Mao–Bell-type diamond anvil cell (DAC), using Be as the gasketing material. In addition to the two openings drilled parallel to the diamond axis, the DAC presents four conical openings lying in the gasket plane, mostly useful for x-ray emission detection. To reach pressures up to the megabar region, we used 1 mm thick gaskets machined in high-strength Be. The thick gaskets are pre-indented with a conical shape, leaving out only a thin part in the centre, whose diameter approximately matches the diamond culet size. The sample is then loaded with ruby chips after indentation and drilling of the central part to a diameter of about 100 μm. Pressure is estimated using the conventional ruby fluorescence technique.

The x-ray emission spectra were measured using the spectrometer installed on ID16. The XES spectrometer is of Rowland circle geometry type with a 1 m diameter. The spectrometer consists of a spherically bent Si analyser working in Bragg reflection and a Peltier-cooled Si diode detector. The Rowland circle geometry imposes the analyser bending radius corresponding to the spectrometer diameter. The x-ray emission spectra are recorded by scanning the analyser Bragg angle while, at the same time, the detector is translated perpendicularly to the analyser direction, following the displacement of the x-ray spot. In order to minimize the source size contribution to the overall spectrometer resolution, we selected analysers having the highest Bragg angle for a given emission line energy. The analyser specifications are summarized in table 1. All the emission spectra were measured at an incident energy of 15 keV, except for NiO as explained in section 2.3.3.

2.2. Cell geometry and self-absorption effects

The cell geometry is dictated by the absorption of the diamonds, particularly strong along the exit path—the emitted energies fall within the 6.4–8.2 keV energy range, whereas the incident energy can be set much higher, 15 keV in the present case—which makes it difficult to work in full transmission geometry, where both incident and emitted x-rays go through the diamonds. Since diamond transmission at 8 keV falls to 3%, and Be only absorbs 30% at the same energy,

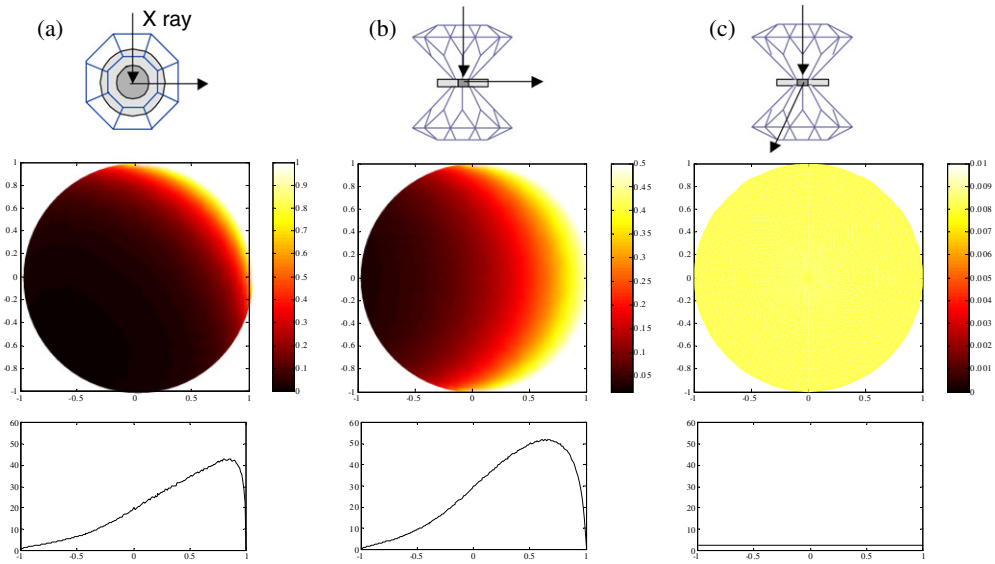

Figure 1. The self-absorption effect in a model transition-metal oxide sample contained in a pressure cell. From top to bottom, sample geometry (a), in-plane scattering (b), perpendicular geometry, (c) full transmission (the sample and the gasket are shown in grey); 2D emission profile; integrated intensity. The sample diameter is 100 μm, and we considered an attenuation length of 30 μm, typical of metal oxides around 8 keV.

Table 1. Measured XES emission lines and analysers.

Sample	Kβ energy (eV)	Analyser	Bragg angle (deg)	Attenuation length at the Kβ energy (μm)
MnO	6490.4	Si(440)	84.1	37
CoO	7649.4	Si(620)	70.7	29
NiO	8264.6	Si(551)	80.4	41

it would be quite natural to let the incident and emitted x-rays be scattered in the Be gasket plane. However, as we will now discuss, one has to take into account the self-absorption of the emitted x-rays.

Self-absorption occurs because the Kβ emission line lies close to the metal absorption K edge, though about 50 eV lower in energy. The x-rays emitted on one part of the sample are partly re-absorbed by the opposite part. The self-absorption strength depends on the sample total length projected along the detection direction, here the sample–analyser axis, and the x-ray attenuation length for the material considered (see table 1). The 2D intensity profile emitted by the sample is shown in figure 1 for different detection geometries: (a) in-plane scattering through the Be gasket, (b) 'perpendicular' geometry (the incident x-ray enters the cell through diamond and exits through the Be gasket) or (c) full transmission through the diamonds. The simulation was carried out by considering a sample of diameter 100 μm placed in an incident x-ray beam of 15 keV, and an attenuation length of 30 μm, conforming to the value found at the Kβ emission line energy in the transition-metal oxides considered (see table 1). As expected, the highest peak intensity is obtained for the in-plane configuration, but because both incident and emitted x-rays are strongly absorbed, only a corner covering about a third of the sample surface is visible from the analyser point of view. In the perpendicular configuration, the

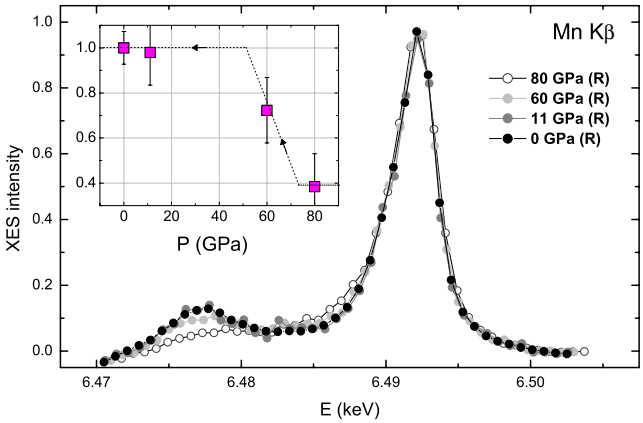

Figure 2. X-ray emission spectra of MnO as a function of pressure. (R) indicates spectra measured upon pressure release. The variation of the satellite intensity is shown in the inset. Arrows indicate the cycling direction.

fluorescence comes from approximately half of the sample. Even if the first diamond absorbs part of the incident beam, the integrated intensity is comparable to the in-plane configuration thanks to the wider emitting area. Finally, a homogeneous sample can be obtained in the full transmission mode, but then the emitted intensity is strongly absorbed by the exit diamond, resulting in a loss of intensity by a factor of $\approx$30. The perpendicular geometry therefore appears to give the best compromise between integrated intensity and sample homogeneity, as long as the sample size is kept small compared the attenuation length and hydrostaticity preserved throughout the entire pressure range. This is also the configuration that we opted for here.

2.3. High-pressure x-ray emission results

2.3.1. MnO. At ambient conditions, MnO crystallizes in the rhombohedrally distorted rock-salt structure (rB1) [13]. Mn has a $3d^5$ electronic configuration ($t_{2g}^3 e_g^2$) in the high-spin state. Among the transition-metal series, Mn has the highest spin moment ($S = 5/2$), and one expects the satellite to be well separated from the main peak of the Kβ line, according to the rule of thumb provided in [11, 12].

The pressure dependence of the Kβ emission line of MnO is shown in figure 2. The spectra were taken upon pressure release from 80 GPa to ambient pressure and normalized to the main peak intensity. The satellite structure is well defined at low pressure but shows a dramatic decrease at 80 GPa, denoting the transition from the high-spin to the low-spin configuration, while the 60 GPa spectrum is intermediate. The pressure at which the transition occurs is better defined by representing the pressure dependence of the satellite intensity (see the inset to figure 2). Remarkably, the satellite presents a sizable intensity in the high-pressure phase. Indeed, in the low-spin state, Mn is in a $t_{2g}^5 e_g^0$ configuration, with a spin $S = 1/2$. Thus in the atomic picture, the spin magnetic moment persists in the high-pressure phase, and the magnetic collapse is not complete. The transition pressure is consistent with the structural change reported for MnO around 90 GPa from the rB1 to the nB8 structure [13].

2.3.2. CoO. At ambient pressure, CoO crystallizes in the non-distorted B1 structure (according to recent diffraction data, a rhombohedral distortion (rB1) was observed above

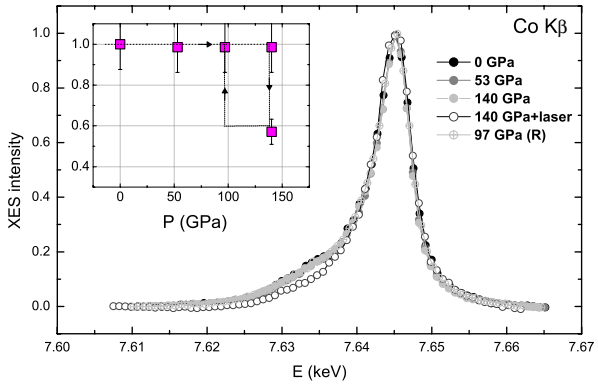

Figure 3. X-ray emission spectra of CoO as a function of pressure. The variation of the satellite intensity is shown in the inset. Arrows indicate the cycling direction.

43 GPa [14]). Similarly to Mn in MnO, Co in CoO has a divalent character but with a $3d^7$ ($t_{2g}^5 e_g^2$) high-spin configuration at ambient conditions, and a total spin magnetic moment equal to $S = 3/2$. As presented in figure 3, the satellite in the XES spectra is now less marked compared to the MnO case, and lies closer to the main peak. Starting from ambient, the pressure was slowly increased up to 140 GPa without noticeable change in the satellite intensity, which is shown in the inset. At this pressure, the sample was laser heated with a Nd:YAG laser and placed back into the spectrometer. Laser heating can release the stresses that accumulate more particularly at these extreme pressures, blocking the magnetic transition. The new XES spectrum obtained after laser heating is characteristic of a low-spin state. Once pressure was released, the high-spin state configuration was retrieved around 97 GPa with a satellite intensity comparable to that of the low-pressure points. The magnetic collapse is likely to be responsible for the contraction of the volume cell, recently reported from x-ray diffraction studies [14] at the transition from the rB1 phase to a high-density rhombohedral phase around 90 GPa. The total variation of the ratio of the satellite to the main peak intensity throughout the complete cycle in CoO is reduced compared to that for MnO, from 60% for the latter sample to 40% for the former. This is consistent with the expected total spin change in CoO of $\Delta S = 1$ from the high-spin to the $S = 1/2$ low-spin configuration ($t_{2g}^6 e_g^1$), with respect to the $\Delta S = 2$ total variation in MnO across the transition.

2.3.3. NiO. The NiO measurements were carried out during a previous run of beam time at ESRF using the same set-up as for MnO and CoO, but in the course of a resonant x-ray emission experiment under high pressure [15]. Because the incident energy had to be tuned to the Ni K edge region, we chose the in-plane geometry in order to avoid the strong attenuation due to the entrance diamond; the diamond transmission changes by a factor of 15 when the energy is decreased from 15 to 8 keV. In the same way, the XES spectra presented here differ from the pure fluorescence one since they were measured on resonance at the maximum of the Ni K edge. Although the overall spectral shape is very similar to the fluorescence spectrum, the ratio of the main peak to the satellite intensity may slightly differ from the off-resonance regime. However, this does not affect the interpretation of the data.

Like MnO, NiO has an rB1 structure at ambient pressure. This structure was found to be stable up to 140 GPa, without any structural changes [16]. Ni in NiO has a $3d^8$ configuration ($t_{2g}^6 e_g^2$) and a total magnetic spin moment of $S = 1$. Interestingly, Ni has the same electronic configuration and magnetic moment in the low-spin state. The XES spectra should therefore

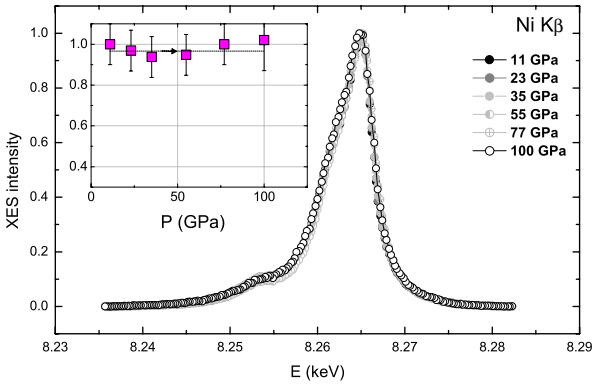

Figure 4. X-ray emission spectra of NiO as a function of pressure. (R) indicates spectra measured upon pressure release. The variation of the satellite intensity is shown in the inset. Arrows indicate the cycling direction.

remain unchanged with pressure variation. The series of normalized spectra measured at pressures ranging from ambient to 100 GPa are plotted in figure 4 and the satellite intensity is shown in the inset. Almost no variation of the XES spectra or satellite intensity is noticeable within the error bars. The absence of observable changes in the Ni XES spectra of NiO under pressure may therefore be ascribed either to the stability of the spin magnetic moment at the transition ($\Delta S = 0$) or to the persistence of a high-spin magnetic state up to 100 GPa, as the diffraction results preferentially suggest. A careful look at the spectra does reveal a slight modification of the spectral lineshape for the two highest-pressure points, which shows up as a weak increase of spectral weight in the satellite region. Rather than suggesting a magnetic transition, we ascribe this to the coupling between the absorption and emission processes on resonance in correlation with the small shift of the Ni K edge that we observed above 55 GPa [15]. Such a shift is likely to be related to partial delocalization of the d electron in the megabar pressure region, as discussed in section 3.1.

3. Discussion

The results exposed in section 2.3 are qualitatively well accounted for by simple arguments regarding the transition-metal electronic configuration in a purely atomic approach. In this approach, we left aside the likely distortion of the metal site, which accompanies the rhombohedral distortion of the unit cell. More importantly, we did not consider electron correlation or charge transfer effects, although both constitute fundamental parameters of the metal oxide electronic properties. More realistic approaches are therefore needed that could embrace this complex electronic picture.

Recently, Cohen *et al* applied an *ab initio* approach to the Mott transition in the metal oxides under high pressure [17]. The calculations were carried out for the simple transition-metal oxides, among them MnO, CoO and NiO, within the local density approximation (LDA) including gradient corrections (GGA). The magnetic collapse is understood in this framework as the gradual delocalization of d electrons as pressure is increased until the Stoner criterion for itinerant magnetism is not fulfilled any longer. However, because of the extreme complexity of *ab initio* calculation for these systems, substantial simplifications had to be used; in particular, the electron correlation was neglected. In other words, the condition $U/W \ll 1$ was considered to hold, at least in the high-pressure regime, so that the LDA band approach would remain

Table 2. Parameters of the configuration interaction model (see the text for details).

				Relative energy (weight)		
P (GPa)	U (eV)	Δ (eV)	$V(e_g)$ (eV)	$3d^8$	$3d^9\underline{L}$	$3d^{10}\underline{L}^2$
11	7.3	2.4	2.1	0 (0.13)	−6.5 (0.66)	−6.0 (0.21)
100	7.6	1.7	2.4	0 (0.12)	−6.3 (0.64)	−5.0 (0.24)

valid. In spite of these simplifications, a magnetic collapse is found to occur in MnO, CoO and NiO at pressures of 150, 90 and 230 GPa respectively. The transition pressure is in reasonable agreement with the experimental values for CoO, but is far too high for MnO; the predicted pressure for NiO is not within the reach of the DAC. Besides this, as mentioned in the introductory part, the insulating state in metal oxides is controlled by ΔW rather than by U/W, and the charge transfer process has to be taken into account in any realistic modelling of these systems.

3.1. Full multiplet calculations

In an attempt to reconcile the atomic picture with the band calculations, both inadequate for treating strongly correlated d electrons, we have recently started making calculations of the XES spectra of the metal oxides using a full multiplet approach. The parametric calculations include correlation and charge transfer energies as parameters as well as the p–d hybridization strength V. Details of the calculations will be published elsewhere. As an example, we present here results for NiO at 11 and 100 GPa.

The calculations were performed using a configuration interaction scheme within a charge transfer multiplet model [18]. Then, the initial, intermediate and final states are represented by a linear combination of $3d^{n+m}\underline{L}^m$ electronic configurations, where $\underline{L}$ stands for the O 2p ligand hole state. The Kβ process for the Ni^{2+} ion is described by the transition between $1s^1 3d^8 + 1s^1 3d^9\underline{L} + 1s^1 3d^{10}\underline{L}^2$ and $3p^5 3d^8 + 3p^5 3d^9\underline{L} + 3p^5 3d^{10}\underline{L}^2$ configurations. We assumed that the initial state is fully relaxed, and that the octahedral symmetry is retained at high pressure. In O_h symmetry, the mixing parameters for e_g and t_{2g} symmetry states are related through $V(e_g) = 2V(t_{2g})$ [19]. The charge transfer energy is defined as $\Delta \equiv E(d^{n+1}\underline{L}) - E(d^n)$, and the d–d electron correlation U as $U \equiv E(d^{n-1}) - E(d^{n+1}) - 2E(d^n)$, where $E(d^nL^m)$ is centre of gravity of the $3d^{n+m}\underline{L}^m$ configuration. The Slater integrals are scaled down to 70% of their single-configuration values in order to account for intra-atomic configuration interaction effects.

The parameters used in the calculations for the two pressures are listed in table 2. The parameters are adjusted to fit the experimental spectra. The calculated spectra are further convoluted with a Lorentzian of 1.4 eV FWHM to take into account the core hole lifetime broadening effect and a Gaussian of FWHM = 1.6 eV to simulate the finite experimental resolution. In a first approximation, the core hole potentials were assumed to be independent of pressure. Also the Slater integrals are scaled down to same value at both pressures. Only the charge transfer energy and the d–d interaction together with the hybridization strength are allowed to change as pressure is increased. The calculated spectra are shown in figure 5 superimposed on the experimental results. The spectra were normalized to the maximum intensity and aligned according to the main peak position. The agreement is satisfactory.

When comparing the parameters for the two pressure points in table 2, we note that both the correlation U and hybridization V are increased when going from low to high pressure, while Δ diminishes. Massey *et al* argue that hybridization in NiO must increase according

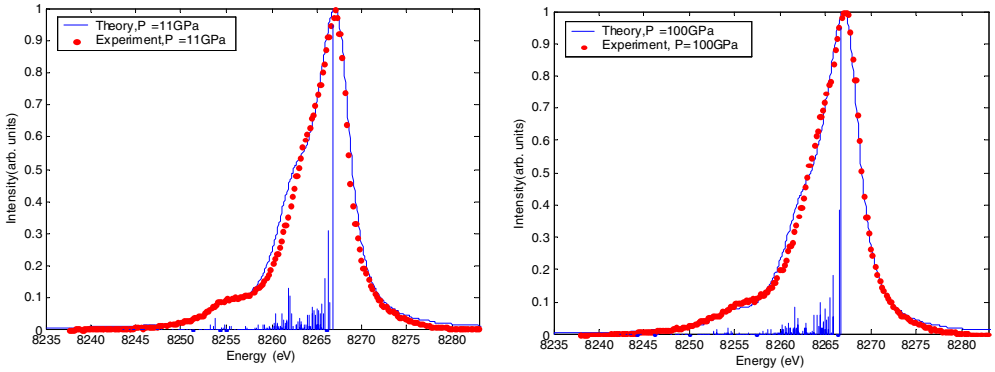

Figure 5. Raw (ticks) and convoluted (solid curve) calculated spectra of NiO at 11 and 100 GPa. The calculations are compared to the experimental results (dots).

to $V \propto a^{-6}$ [20]. The reported change in the lattice parameter $\Delta a/a \approx -7 \times 10^{-2}$ [16] between 11 and 100 GPa should lead to an increase of hybridization strength of about 0.8 eV. Although the growth of hybridization with pressure is confirmed here, we observe a change of V on a smaller scale. On the other hand, one expects the correlation energy to weaken as the system goes more metallic at high pressure because of the more efficient screening, in contradiction to the calculated values. Nevertheless, since the measurements were done on resonance, it is likely that the variation of U is dominated by the interplay between the absorption and emission processes. Thus, interpretations in terms of pressure-induced change in the electronic correlations remain uncertain at this point. Finally, the charge transfer energy Δ is observed to decrease with pressure. Previous works on CuO compounds [21] pointed out that a charge transfer-type insulator such as NiO, characterized with a p–d-type band gap, may give rise to a p–p-type insulator as Δ is decreased. This could provide a rationale for the modification of the XES (and absorption) spectral lineshape observed at high pressure in NiO.

On way of improving the simulation would be to relax the constraint on the O 2p bandwidth, kept constant in the present calculations. Preliminary results on the calculated XES spectra of MnO and CoO under pressure across the magnetic transition indicate that both the crystal field strength and the O 2p bandwidth have to be changed to reproduce the experimental spectra. It would be interesting to carry out a similar analysis for other transition-metal compounds to assess the interdependence of those two parameters.

4. Conclusions

We have studied the magnetic collapse in a series of simple transition-metal oxides under very high-pressure conditions by x-ray emission spectroscopy. In MnO and CoO, a magnetic collapse was observed from a radical change in the Kβ emission lines, at pressures of 80 and 90 GPa respectively. In contrast, the NiO magnetic state remains stable up to 100 GPa, though with some indications of a partial delocalization of the d electrons. The Ni emission spectra were simulated using a full multiplet approach. The spectra can be well reproduced, although improvements in the choices of the parameters are necessary.

XES appears to be complementary to existing probes of electronic and magnetic properties, such as the nuclear probes and magnetic dichroism, with the advantages of simplicity (no magnetic field) and versatility (no isotope substitution). XES is particularly well suited for

dealing with samples in heavily constrained environments such as high-pressure systems, catalytic cells and high-temperature systems.

Acknowledgment

The authors are indebted to F M F de Groot for fruitful assistance in the multiplet calculations for NiO.

References

[1] Imada M, Fujimori A and Tokura Y 1998 *Rev. Mod. Phys.* **70** 1039
[2] Mott N 1968 *Rev. Mod. Phys.* **40** 677
[3] Pasternak M, Taylor R, Chen A, Meade C, Falicov L, Giesekus A, Jeanloz R and Yu P 1990 *Phys. Rev. Lett.* **65** 790
[4] Xu W, Naaman O, Rozenberg G K, Pasternak M and Taylor R 2001 *Phys. Rev.* B **64** 94411
[5] Lengsdorf R, Ait-Tahar M, Saxena S S, Ellerby M, Khomskii D I, Micklitz H, Lorenz T and Abd-Elmeguid M M 2004 *Phys. Rev.* B **69** 140403(R)
[6] Odin S, Baudelet F, Giorgetti C, Dartyge E, Itié J P, Polian A, Chervin J C, Pizzini S, Fontaine A and Kappler J P 1999 *Europhys. Lett.* **47** 378
[7] Ishimatsu N, Maruyama H, Kawamura N, Suzuki M, Ohishi Y, Ito M, Nasu S, Kawakami T and Shimomura O 2003 *J. Phys. Soc. Japan* **72** 2372
[8] Rueff J-P, Kao C, Struzhkin V V, Badro J, Shu J, Hemley R and Mao H 1999 *Phys. Rev. Lett.* **82** 3284
[9] Badro J, Struzhkin V, Hemley R, Mao H-K, Kao C-C, Rueff J-P and Shen G 1999 *Phys. Rev. Lett.* **83** 4101
[10] Badro J, Fiquet G, Guyot F, Rueff J-P, Struzhkin V, Vankó G and Monaco G 2003 *Science* **300** 789 (published online 10.1126/science.1081311)
[11] Tsutsumi K, Nakamori H and Ichikawa K 1976 *Phys. Rev.* B **13** 929
[12] Peng G, de Groot F M F, Hämäläinen K, Moore J, Wang X, Grush M, Hastings J, Siddons D, Amstrong W, Mullins O and Cramer S 1994 *J. Am. Chem. Soc.* **116** 2914
[13] Fang Z, Solovyev I, Sawada H and Terakura K 1999 *Phys. Rev.* B **59** 762
[14] Guo Q, Mao H, Hu J, Shu J and Hemley R 2002 *J. Phys.: Condens. Matter* **14** 11369
[15] Shukla A, Rueff J-P, Badro J, Vanko G, Mattila A, de Groot F M F and Sette F 2003 *Phys. Rev.* B **67** 81101
[16] Eto T, Endo S, Imai M, Katayama Y and Kikegawa T 2000 *Phys. Rev.* B **61** 14984
[17] Cohen R, Mazin I and Isaak D 1997 *Science* **275** 654
[18] de Groot F M F 2001 *Chem. Rev.* **101** 1779
[19] Mattheiss L 1972 *Phys. Rev.* B **5** 290
[20] Massey M, Chen N, Allen J and Merlin R 1990 *Phys. Rev.* B **42** 8776
[21] Mizokawa T, Namatame H, Fujimori A, Akeyama K, Kondoh H, Kuroda H and Kosugi N 1991 *Phys. Rev. Lett.* **67** 1638